

Uplift history of the northern Sierras Pampeanas broken foreland using river profile modelling

Julieta C. Nobile* and Federico M. Dávila

CICTERRA-CONICET, Centro de Análisis de Cuencas, Universidad Nacional de Córdoba.

*Contact email: jnobile@efn.uncor.edu

Abstract. Different geological and geophysical approaches have suggested that the Argentine broken foreland (Sierras Pampeanas) uplifted after ~5 Ma, with higher amounts to the north respect to the south. But the information comes from a poorly constrained stratigraphy. The lack of dated marker beds and low-temperature thermochronology has supplied no conclusive results. In this contribution we use a longitudinal river profile analysis to give insight into the uplift history of the N Sierras Pampeanas (Aconquija-Ambato ranges). The method is based on an inverse algorithm that relates river profiles with uplift rates. Our results show two main uplift peaks that would have occurred <20-15 Ma, which matches with geological data.

Keywords: longitudinal river profile, Sierras Pampeanas, uplift history.

1 Introduction

The Sierras Pampeanas of Argentine (FIGURE 1A) has been interpreted as a “broken foreland” and world analogue (Jordan and Allmendinger, 1986) for forelands affected by flat subduction (e.g. US Laramides). Recent works have also suggested that the longest wavelength elevations across and along strike were also driven by flat slab dynamics (Dávila and Lithgow-Bertelloni, submitted). This scenario is, consequently, ideal to study the interaction between surface morphology, tectonics and geodynamics.

The Sierras Pampeanas, nevertheless, is not a homogeneous basement-thrusting province -as largely assumed- and the amount and timing of surface uplift vary along and across strike.

In this contribution we calculate the uplift history and uplift rates by using a river profile inverse algorithm (Pritchard et al., 2009 and Roberts and White, 2010). We contrast our modeling results with independent geologic observations and AFT forward modeling (Ketcham, 2005). The rivers are located in the eastern gentler slope of the Aconquija-Ambato range, between 27°- 27° 55' SL and 66° 25'-65° WL. These streams are part of Medinas river drainage network. The headwaters are place in the Valle del Pucará (1600 m.s.l.) and the Sierra de Aconquija (5550 m.s.l.) whereas the Medinas river is a tributary of the Río Chico which drains to the Tucumán Valley (260 m.s.l.) (FIGURE 1).

2 Methodology and Results

2.1 Stream power erosion law

In regions of active uplift, the concave-up longitudinal profile morphology modifies as the river gradient readjusts toward new equilibrium conditions, when the relative base level also changes. The resulting surface uplift (defined as the upward movement of the landsurface with respect to a specific datum) can be determined by combining denudation rate and crustal uplift. The “stream power erosion law” states that local erosion rate is a power-law function of the drainage area (A) and stream gradient (S) (Howard and Kerby, 1983). Then a river profile dynamics can be written as (Whipple et al., 1999, Howard et al. 1994):

$$\frac{\partial z}{\partial t}(x, t) = U(x, t) - E(x, t) = U(x, t) - KA^m S^n \quad (1)$$

Where $\partial z/\partial t$ is the rate of change of bed elevation, $U(x,t)$ is rock uplift rate, $E(x,t)$ is the mean erosion rate, k is a dimensional coefficient of erosion, m and n are positive empirical area and slope coefficients (Howard and Kerby, 1983, Whipple and Tucker, 1999). Roberts and White (2010) used these equations to calculated uplift rate histories and we used the same approach to analyze the Argentine broken foreland uplift.

2.2 Model details

In their forward model Roberts and White (2010) represents erosion (E) as a combination of advection and diffusion:

$$\frac{\partial z}{\partial x} = U(t) - v_0 x^m \left(-\frac{\partial z}{\partial x} \right)^n + \kappa(x) \frac{\partial^2 y}{\partial x^2} \quad (2)$$

and then developed an inverse model which estimates a hypothetical uplift rate history, $U(t)$ that best fit the observed river profile. In equation (2) v_0 is the knickpoint velocity, m the distance exponent; κ is the diffusive coefficient of erosion and n the slope exponent. We run 5 tests to select an adequate combination of the erosional parameters m , n and v (taken from Roberts and White, 2010. TABLE 1). The most appropriate combination of

erosional parameters was chosen by contrasting geologic information and exhumation analysis (Coughlin, 2000; Dávila, 2011).

The drainage network and river profiles were calculated with a flow routing algorithm from the Aconquija range (~27° SL) downstream to the Tucumán Valley (considered the local base level, 269 m.s.l.) (FIGURE 1). River profiles were extracted using ESRI ArcGIS® software tools.

Table 1. Erosional parameters and units used in this Study.

	Test <i>a</i>	Test <i>b</i>	Test <i>c</i>	Test <i>d</i>	Test <i>e</i>	Units
κ	10 ⁵	10 ⁵	10 ⁵	10 ⁵	10 ⁵	m ² Myr ⁻¹
<i>n</i>	1.0	1.0	1.0	1.0	1.0	dimensionless
<i>m</i>	0.5	0.5	0.7	0.7	1.2	dimensionless
<i>v</i>	50.0	4.75	3.8	0.125	0.0125	m ^(1-m) Myr ⁻¹

Results and conclusions

Considering a slope exponent $n=1$, the erosion along the rivers profiles is dominated by knickpoint retreat, and the knickpoint velocity is controlled by $v\kappa^m$. Analyzing the uplift amount results, the best combination of erosional parameters corresponds to the tests *a* and *c*, which show an uplift onset at ~15 and ~20 Ma (FIGURE 2). In contrast, tests *b*, *d* and *e* show maximum uplift amount reached before 20 Ma and therefore were rejected. Apatite fission track analysis of basement rocks from Coughlin et al. (1998), re-analyzed in this study, indicate a long period in which apatites resided in the PAZ (120-60° C) before 20 Ma, and a rapid uplift cooling event after 20 Ma. This also agrees with the tests *a* and *c*.

Our prefer models (*a* and *c*) show two major uplift events that took place at Miocene times. While test *a* shows a much younger event, with 2 uplift peaks at ~12 Ma and ~7 Ma, test *c* has two major peaks at ~20 Ma and ~10 Ma. According to the available stratigraphy (Dávila et al., 2012), we incline toward the model *a*, which is also coherent with the major deformation and geodynamic events occurred along the northern Sierras Pampeanas (e.g., Strecker et al., 2009).

References

Coughlin, T.J. 2000. Linked orogen-oblique fault zones in the Central Andes: implications for Andean orogenesis and metallogenesis (Unpublished), University of Queensland, Queensland: 268 p.

Coughlin, T.J.; O'Sullivan, P.B.; Kohn, B.P.; Holcombe, R.J. 1998. Apatite fission-track thermochronology of the Sierras Pampeanas, central western Argentina: Implications for the mechanism of plateau uplift in the Andes. *Geology* 26: 999-1002

Dávila, F.M.; Giménez, M.E.; Nóbile, J.C.; Martínez, M.P. 2012. The evolution of the high-elevated depocenters of the northern Sierras Pampeanas (ca. 28° SL), Argentine broken foreland, South-Central Andes: the Pípanaco Basin. *Basin Research* 24: 1-22.

Dávila, F.M. 2011. Revisión de edades de enfriamiento de baja temperatura en las Sierras Pampeanas (26°-34° SL). In XVIII Congreso Geológico Argentino, Actas S12: 733-734. Neuquén.

Howard, A.D.; Kerby, G. 1983. Channel changes in badlands. *GSA Bulletin* 94: 739-752.

Howard, A. D.; Seidl, M. A.; Dietrich, W. E. 1994. Modeling fluvial erosion on regional to continental scales. *J. Geophys. Res.* 99: 13971-13986.

Jordan, T.E.; Allmendinger, R.W. 1986. The Sierras Pampeanas of Argentina: A modern analogue of Rocky Mountain foreland deformation. *American Journal of Science* 286: 737-764.

Ketcham, R.A. 2005. Forward and inverse modeling of low-temperature thermochronometry data. In *Low Temperature Thermochronology: Techniques, Interpretations, and Applications* (Reiners, P.W., Ehlers, T.A.; eds.). Mineralogical Society of America, 275-314. Washington D.C

Ketcham, R.A.; Carter, A.C.; Donelick, R.A.; Barbarand, J.; Hurford, A.J. 2007. Improved modeling of fission-track annealing in apatite. *Am. Mineral.* 92: 799-810.

Pritchard, D.; Roberts, G.G.; White, N.J.; Richardson, C.N. 2009. Uplift histories from river profiles. *Geoph. Res. Letters* 36: L24301.

Roberts, G.G.; White, N.J.; 2010. Estimating uplift rate histories from river profiles using African examples. *J. Geophys. Research* 115: B02406.

Strecker, M.R.; Alonso, R.; Bookhagen, B.; Carrapa, B.; Coutand, I., Hain, M.P.; Hilley, G.E.; Mortimer, E.; Schoenbohm, L.; Sobel, E.R. 2009. Does the topographic distribution of the central Andean Puna Plateau result from climatic or geodynamic processes? *Geology* 37: 643-646.

Whipple, K.X.; Tucker, G.E. 1999. Dynamics of the stream-power river incision model: Implications for height limits of mountain ranges, landscape response timescales, and research needs. *J. Geophys. Research* 104(B8): 661-674.

Whipple, K.X.; Kirby, E.; Brocklehurst, S.H. 1999. Geomorphic limits to climate-induced increases in topographic relief. *Nature* 401: 39-43.

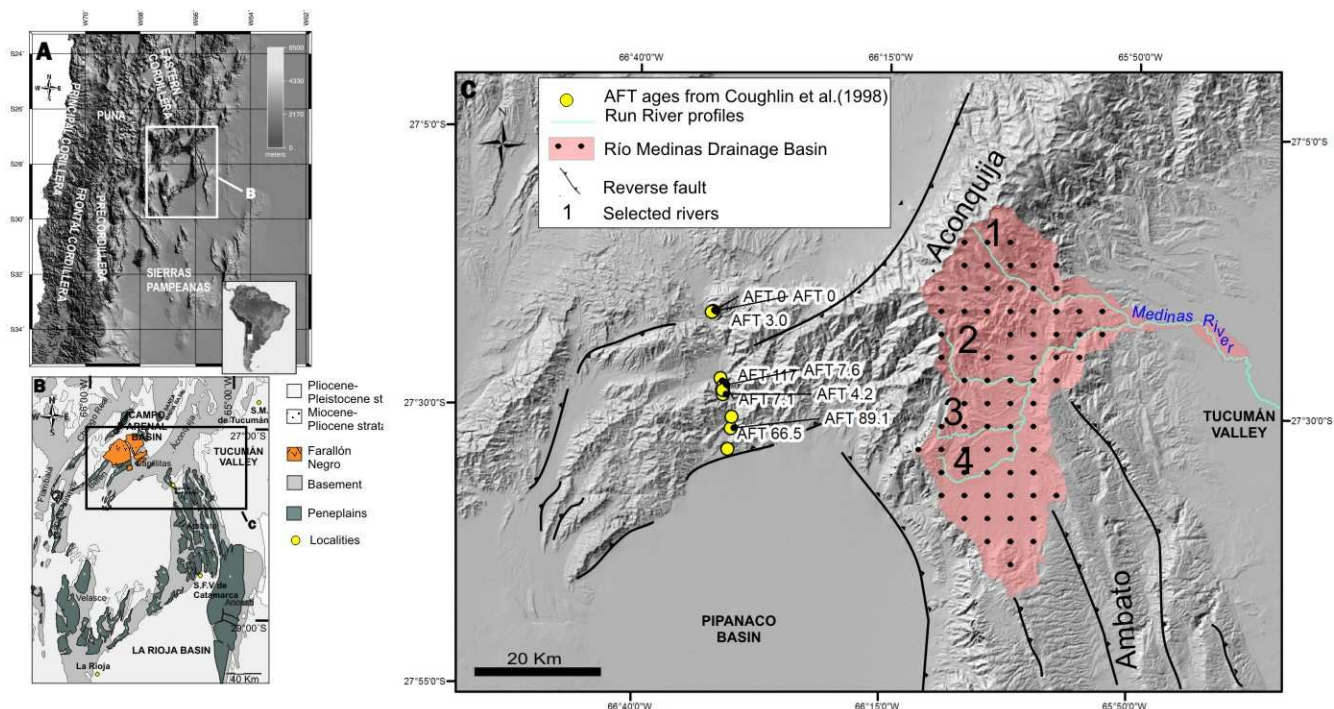


Figure 1. A Digital elevation model of the study area and morphotectonic domains (shown on inset) **B** Geological map of the N Sierras Pampeanas region. **C** DEM hillshade with study drainage basin, rivers analyzed and AFT ages location (Coughlin et al. 1998).

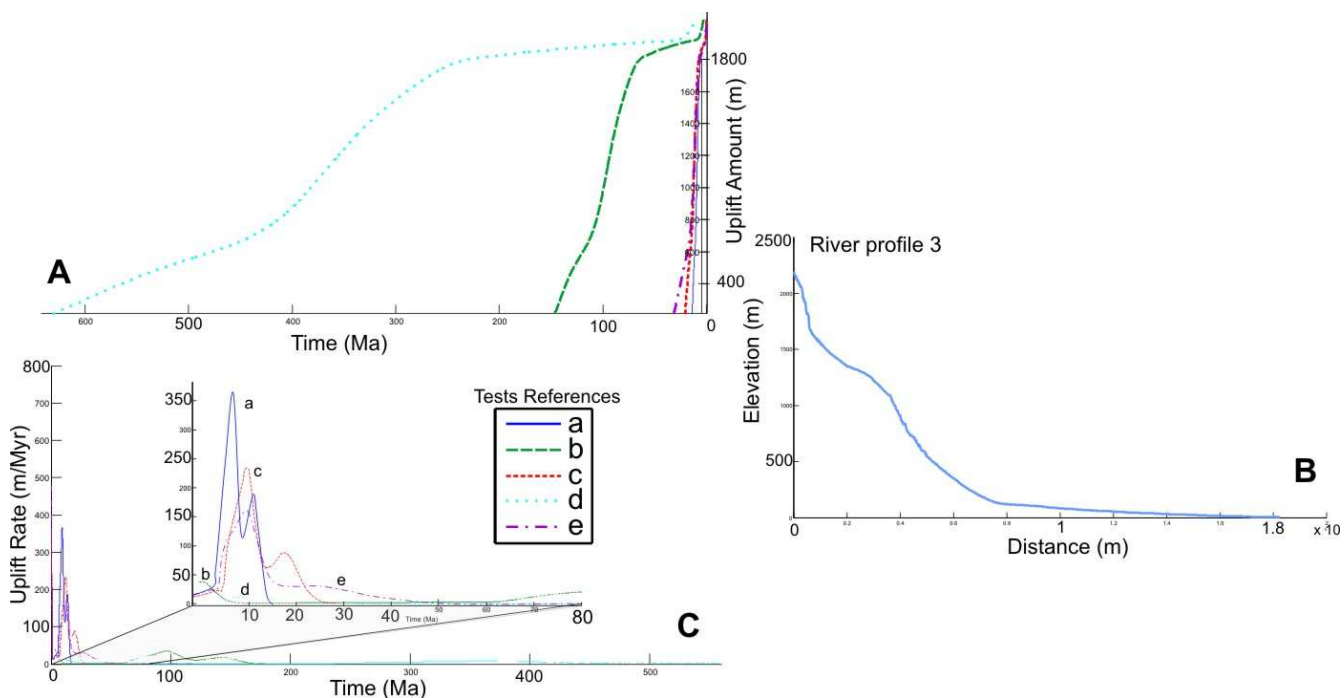


Figure 2. An example of the inverse algorithm results showing the accumulated uplift rate history (A) and the Uplift Rate (C) from one longitudinal river profile from source to mouth (B) analyzed.